

1 Fast imaging of millimeter-scale areas with beam deflection 2 transmission electron microscopy

3
4 Zhihao Zheng¹, Christopher S. Own², Adrian A. Wanner^{1,3}, Randal A. Koene², Eric W.
5 Hammerschmidt¹, William M. Silversmith¹, Nico Kemnitz¹, David W. Tank¹, H. Sebastian
6 Seung^{1,†}

7
8 ¹Princeton Neuroscience Institute, Princeton University, Princeton, NJ, USA

9 ²Voxa, Seattle, WA, USA

10 ³Present address: Paul Scherrer Institute, Villigen, Switzerland

11 [†]Correspondence to sseung@princeton.edu

13 Abstract

14 We have achieved a three fold increase in the speed of transmission electron
15 microscopy by using a beam deflecting mechanism to enable highly efficient acquisition of
16 multiple image tiles for each motion of the mechanical stage. For millimeter-scale areas, the
17 duty cycle of imaging doubles and exceeds 30%, yielding a net average imaging rate of 0.3
18 gigapixels per second.

20 Main text

21 Volume electron microscopy (EM) is currently the only approach that has been used to
22 reconstruct a connectome – a complete map of neural connectivity at synaptic resolution. Serial
23 section transmission electron microscopy (ssTEM) is a classic volume EM technique used for
24 3D reconstruction of neural tissues at small scale¹⁻³. In the 1980s, ssTEM was used for
25 mapping the first whole-brain connectome of *C. elegans*⁴. Later on, ssTEM was used to acquire
26 3D EM datasets of multiple *C. elegans* brains^{5,6}, an entire fly larval brain⁷, normal and
27 pathological retinas^{8,9}, and mouse cortex^{10,11}. Recently, automation and parallelization of
28 TEM^{10,12,13} have allowed imaging of ever larger volumes, such as a complete adult flybrain¹⁴ and
29 a cubic millimeter volume of mammalian cortex¹⁵.

30
31 The previous state of the art in high throughput TEM was a system at the Allen Institute
32 for Brain Science¹². This achieves high imaging speed through several innovations. A reel-to-
33 reel tape translation system allows automated delivery of sections based on GridTape
34 technology¹³. A 50 MPixel CMOS camera with a low distortion lens achieves a burst imaging
35 rate of 0.5 gigapixels per sec (GPix/s, imaging only). A scalable software infrastructure allows
36 closed-loop workflow management based on real-time image processing¹⁶. However, imaging
37 time for a cubic millimeter volume is still 6 months with multiple TEMs¹² and there is a growing
38 need to image much larger datasets¹⁷.

39
40 Imaging a square millimeter area requires thousands of x-y stage translations to acquire
41 image tiles that are later stitched together to form a multi-tile image. Because the time to image
42 a tile has become so fast the stage translations require more time than the image capture
43 itself¹². A massive number of positional translations – typically ~10,000 per mm² – also rapidly

44 consumes piezo stage life of ~10 billion cycles of the crystal per year when operated 24/7.
45 Therefore, to advance the state of the art, it is essential to reduce the overhead due to stage
46 translations.

47
48 Here we report the development of a beam deflection mechanism (CricketTM) to
49 significantly increase TEM imaging throughput (bdTEM, beam deflection). In addition, the
50 microscopes are integrated with an automated reel-to-reel tape translation system^{12,13} and a 50
51 MPixel CMOS camera¹². The bdTEM achieves the fastest TEM imaging rate to date, a three
52 fold increase over the previous TEM with the same camera¹².
53

54 *Beam deflection (Cricket).* We repurposed electromagnetic lens deflectors in the TEMs,
55 above the object plane and below (Fig. 1a). The deflectors above the object plane shift the
56 electron beam over the specimen in a matrix of 3 x 3 tiles and simultaneously the deflectors
57 below the object plane precisely de-scans the image back onto the TEM camera. The beam
58 deflection allows acquisition of 9 image tiles without moving the stage, eliminating 8 out of 9
59 stage movements (Fig. 1b-c, Extended Data Fig. 1b). Overhead for stage motion is therefore
60 significantly reduced, accounting for only 7% of montage imaging time with an additional 9% of
61 Cricket settling time (Fig. 1d). As a result, the imaging duty cycle increases from a previous
62 peak performance of 15%¹² to over 30% of total time per section in our system (Methods).
63

64 *Optics.* The detector optics of the TEM is upgraded with a compact light-optical lens
65 assembly and a high speed CMOS camera that yields a frame size of 6,000 × 6,000 pixels (or
66 36 MPix). The sensor sits near the film plane of a conventional TEM (Extended Data Fig. 1a),
67 eliminating the impractical need of an extended vacuum column required by the past
68 generations of large pixel-count detectors^{10,12}. Images acquired at an exposure time of 40 ms
69 have sufficient resolution for synapse identification and reconstruction of neuronal morphology
70 (Fig. 1e-i, Supplementary video 3). As a result, the burst imaging rate (0.9 GPix/s, imaging only)
71 of bdTEMs is 1.8 times that of the previous fastest imaging rate¹² (0.5 GPix/s).
72

73 *Section transition and stage.* The TEMs are integrated with a previously reported reel-to-
74 reel tape translation system and a two-axis piezo-driven stage^{12,13}. This reel-to-reel tape
75 translation system allows automated section exchange and barcode-based slot identification
76 using GridTape technology^{12,13}. In previous volume TEM techniques, stage step-and-settle time
77 ranges from under 50 ms to 100 ms for one axis^{12,14}. The stage in our TEMs achieves a step-
78 and-settle time of ~57 ms on average on both axes (Extended Data Fig. 1c-d), increasing
79 efficiency on the remaining stage motions.
80

81 These modifications dramatically increase imaging throughput. Acquisition of a 1 mm²
82 section takes 8.6 minutes including imaging, stage motion, and section transition (net average
83 imaging rate of 0.3 GPix/s at 3 nm/pix, Fig. 1d, Table 1, and Supplementary Video 1). The net
84 imaging rate is 3 times the peak imaging rate of the previous fastest TEM at 0.1 GPix/s with the
85 same 50 MPix camera¹². The previous imaging rate¹² includes overhead for image quality
86 control and post-processing. These functionalities have not yet been integrated into our

87 acquisition software but in principle could be performed during the overhead for acquisition
88 software and section transition.

89

90 We set out to test whether the TEMs can be used to acquire a 3D EM volume. The reel-
91 to-reel sample delivery system requires serial ultrathin sections to be cut and collected on
92 GridTape^{12,13}. Based on previous designs^{12,13}, we modified an ATUMtome (RMC/Boeckeler) to
93 be compatible with an ultramicrotome (Leica UC7) and GridTape, and used the automated
94 sectioning system to collect serial ultrathin sections of mouse hippocampus tissue. Imaging a
95 series of sections involves cycling through the following steps: (1) translate GridTape to the
96 targeted slot guided by index barcodes; (2) acquire an overview image of the section at low
97 magnification (Fig. 1c); (3) extract ROI from the overview image and set imaging parameters
98 (e.g. illumination correction and autofocus); (4) montage imaging of the ROI at high resolution.
99 Basic software has been implemented to run the workflow (Supplementary video 1). With 10%
100 overlap between supertiles and 15% overlap between subtiles within a supertile, all tiles of a
101 common section of 1 mm² in size can be stitched together (Fig. 1e-i). Consecutive sections are
102 aligned to assemble a volume (Supplementary Video 2-3). Ultrastructural features such as
103 postsynaptic densities and vesicles are clearly defined (Fig. 1i). Small-diameter axons and
104 dendrites can be followed across sections. These data demonstrate that sequential sections
105 imaged with the bdTEMs can be assembled into a 3D volume for connectomic application.

106

107 An array of four microscopes have been fully installed in our facility (Extended Data Fig.
108 2), some of which have been reliably acquiring data for many months with reasonable
109 microscope downtime¹². By estimate, if the four bdTEMs are running 24/7, imaging a cubic
110 millimeter will take about a month (Table 1). However, non-stop long-term imaging requires
111 further development of automation software that can handle image quality control, workflow
112 management, image and section databases, and stitching and alignment. A scalable
113 architecture with these functionalities has been developed¹⁶ but needs to be adapted to
114 integrate with bdTEMs. On raw imaging speed, breakdown of various overhead sources (Fig.
115 1d) points to several avenues of future improvements. Upgrade of the optics with a 100 MPix
116 camera will in principle double the burst imaging rate. Additional increase of imaging speed can
117 be gained by refactoring frequently used tasks in the acquisition software to low-level programs,
118 reducing tile overlap, enlarging pixel size, and increasing efficiency on section transition.

119

120 Volume EM is dichotomized into SEM-based and TEM-based methods, and both have
121 been shown to be capable of acquiring large-scale datasets (MultiSEM¹⁸ and GridTape-based
122 TEM¹⁵). Here we have further improved the TEM imaging speed to 0.3 GPix/s. Similar to the
123 previous TEMs^{12,13}, our modifications are based on a retrofitted JEOL 1200EX-II microscope
124 and cost for the entire system (< \$500,000) is significantly lower compared to equivalent
125 imaging systems, permitting acquisition of multiple TEMs for an imaging facility (six at the Allen
126 Institute for Brain Science¹² and four at Princeton University). The current system, however,
127 requires specialized films on GridTape, which scales linearly in cost with the number of sections
128 (USD \$4 - \$8 per slot); but improving film-making methods and economies of scale may
129 decrease the cost in the future. Crucially, both imaging methods currently depend on cutting and
130 collecting a large number of ultrathin sections. Sectioning-related artifacts (folds, cracks, knife

131 marks, etc.) are very common, though automated reconstruction methods that are robust to
132 some defects have been developed^{19,20}. Wide-area milling of imaged tissue was recently
133 developed to circumvent ultrathin sectioning²¹ and, if integrated with a MultiSEM, can potentially
134 scale up connectomic volumes beyond petascale. In addition, the reliability of serial sectioning
135 can be improved by magnetic section collection²². For TEM, one proposal to improve reliability
136 of sectioning is to increase the thickness of serial sections, which are then imaged with
137 tomography to recover a finer axial resolution²³. Whether SEM or TEM-based techniques is the
138 method of choice for exascale datasets remains to be determined.

139

140 Methods

141 **Sample preparation and sectioning.** All procedures were carried out in accordance with the
142 Institutional Animal Care and Use Committee at Princeton University. Mice (C57BL/6J-Tg(Thy1-
143 GCaMP6f) GP5.3Dkim/J, Jackson Laboratories, 028280) aged 6 months were transcardially
144 perfused with a fixative mixture of 2.5% paraformaldehyde and 1.3% glutaraldehyde in 0.1M
145 Cacodylate with 2mM CaCl₂ pH 7.4. The brain was extracted and post-fixed for 36 hrs at 4°C in
146 the same fixative solution. The perfused brain was subsequently rinsed in 0.1M Cacodylate with
147 2mM CaCl₂ for 1 hr (3 x 20 mins) and 300 μm coronal sections were cut on a Leica Vibratome.
148 Sample blocks were cut out and stained based on a modified reduced osmium treatment
149 (rOTO) protocol with the addition of formamide^{15,24}. The tissue blocks were first *en bloc* stained
150 with 8% formamide, 2% osmium tetroxide, 1.5% potassium ferrocyanide for 3 hours.
151 Subsequently, the samples were immersed in 1% TCH (94 mM) 50 °C for 50 mins, followed by
152 a second step of 2% osmium staining for 3 hours. The sample was placed in 1% uranyl acetate
153 overnight at 4°C, followed by lead aspartate (Walton's, 20 mM lead nitrate in 30 mM aspartate
154 buffer, pH 5.5) at 50 °C for 2 hours. After washed with water (3 x 10 mins), samples proceeded
155 through a graded acetonitrile dehydration series (50%, 75%, 90% w/v in acetonitrile, 10 minutes
156 each at 4 °C, then 4 x 10 minutes of 100% acetonitrile at room temperature). After a progressive
157 resin infiltration series (33% resin:acetonitrile, 50% resin:acetonitrile, 66% resin:acetonitrile, 8
158 hours each), the sample was incubated in fresh 100% resin overnight and the resin was cured
159 in the oven at 60 °C for at least 48 hrs.

160 GridTape (Luxel Corporation) contains regularly spaced apertures with plastic film
161 substrates for serial sections^{12,13}. The films are transparent to electrons, and therefore are
162 compatible with TEM imaging. We combined an automated tape collecting system (ATUMtome,
163 RMC/Boeckeler) and an ultramicrotome (UC7, Leica) to create an automated tape-based
164 sectioning and collection system (Automated Tape Collecting Ultramicrotome, ATUM) for
165 GridTape, based on previous designs^{12,13}. Our custom ultramicrotome setup also includes a
166 computer-controlled, high-precision motorized stage, monitoring of temperature and humidity,
167 and three cameras to monitor the collection process. Additionally, we have built closed-loop
168 control software to phase-lock aperture movement with cutting, in order to center sections
169 collected in the apertures on GridTape. After resin embedding, the ultrathin sections were then
170 cut at a nominal thickness of 40 nm and automatically collected onto a GridTape.

171

172 **Reel-to-reel translation system and GridStage.** The reel-to-reel translation system and
173 GridStage (Voxa) have been described previously¹². Briefly, Gridstage Reel comprises three
174 major components: a stage cartridge, a reel storage and delivery system, and an airlock

175 assembly enabling cartridge loading. A 3D rendering of the GridStage Reel system is shown in
176 Extended Data Fig. 1, attached to a JEOL 1200EX-II microscope chassis. GridStage's two-axis
177 stage cartridge is set to a fixed height to enable the imaging environment to stay the same from
178 section to section as they are delivered into the imaging area by conveyor. Each axis is driven
179 by a precision closed-loop piezo motor. The precision is ~50 nm, and absolute positional
180 accuracy on the sample is typically between 100 - 200 nm. This mechanism positions the
181 sample accurately and reliably within the requirements of montage image overlap
182 reproducibility, even given electron-optical environment variability (e.g. charging and sample
183 morphology changes) of different samples in the volume. The cartridge incorporates an
184 accurate barcode reading and clamping mechanism to precisely position and identify slots on
185 GridTape, with read accuracy greater than 99.9% for fresh GridTape. This enables precise
186 tracking of the current tissue section under first-time montage imaging or during re-imaging
187 operations. The precision of the GridStage sample ID subsystem supports either sequential or
188 fully random-access sample delivery modes.

189 The stage has fast responsiveness, with roundtrip communication to the drive system on
190 the order of a few milliseconds, and typical step-and-settle times (>95% of moves) occurring in
191 under 60 ms (Extended Data Fig. 1c-d). The average step-and-settle time is similar to and
192 slightly improved over a previously reported fast Piezo-driven stage¹⁴. Voxa reels are housed in
193 robotic delivery and take-up conveyor systems connected to the microscope's vacuum, and can
194 accept a GridTape reel with up to 5,500 sections spaced 6 mm apart. A continuously-monitored
195 belt tension meter ensures the GridTape translates within specified operating parameters, and
196 supports safe transit of the samples into and out of the imaging area. The GridStage reel
197 sample delivery system can deliver sequential sections as fast as once every two seconds, for
198 quick survey modes.

199
200 **Lens assembly and camera.** The electron optics of each of our TEM systems consists of a
201 custom phosphor scintillator of 75 mm in diameter, a lens assembly (AMT, NanoSprint50M-AV),
202 and a high speed CMOS camera (XIMEA, CB500MG-CM). The pickup area of 47 x 47 mm on
203 the phosphor screen is near the film plane of the JEOL 1200EX-II TEM and therefore minimizes
204 image distortion at the bottom of the column and matches the nominal magnification setting of
205 the microscope platform. Conveniently, this setup eliminates the need for a lengthened column
206 that previously requires building scaffolds and is impractical for many facilities^{10,12,14}. In addition,
207 compared to the previous design of an extended column, the smaller scintillator and compact
208 lens in our TEMs allows good signal-to-noise with lower dose or with shorter exposure times
209 leading to more efficient use of available beam electrons. The CMOS camera has a PCIe
210 interface that supports fast data transfer rates. Overall, the lens and camera supports nominal
211 image acquisition with a frame size of 6,000 x 6,000 pixels at a shortest exposure time of 40 ms.
212 In the future, an upgrade of a 100+ Mpix CMOS camera with backside illumination could
213 potentially lead to another couple-fold increase of imaging rate¹².

214
215 **TEM imaging.** Some components of the TEM systems have been briefly presented before²⁵.
216 The Beam deflection mechanism (Cricket) for TEM has been prototyped previously¹² but not
217 demonstrated for large-scale imaging. For imaging, a reel containing samples on a GridTape
218 are first loaded into the reel housing of the reel-to-reel system (Extended Data Fig. 1), which is

219 connected with the TEM column vacuum. After loading, the microscope is pumped down to
220 reach the vacuum level of ~1E-7 Torr. Lanthanum hexaboride crystal (LaB₆) filaments were
221 used due to their high electron flux per unit area and a longer lifetime (1,000 hrs or more as
222 opposed to 200 hrs for a tungsten source) reducing downtime needed for filament change.
223 Crucially LaB₆ filaments depend more sensitively on a good vacuum pressure for good stability
224 and lifetime (low 10⁻⁷ Torr). It typically takes about half a day when loading a new sample reel to
225 pump down the column to the base operating pressure for LaB6. We then increase the high-
226 tension voltage to 120 KV, turn on filament current and then perform alignments on various
227 components of the TEM, following routine technical instructions for TEM operations. These
228 procedures take half a day and only need to be performed after installation of a new filament or
229 loading of a new tape. Calibration of reel-to-reel systems involves tape and tension calibration
230 for reliable translation and barcode reading, which typically takes ~5 minutes and is only done
231 when first loading a reel. Cricket alignment is performed to ensure each sub-tile has sufficient
232 overlap (~15%) with neighboring sub-tiles and that there is minimal distortion across the field
233 between images from different sub-tiles to facilitate efficient stitching and reconstruction. Cricket
234 alignment is usually stable over several months.

235 The TEMs are compatible with GridTape¹³, which has regularly spaced 2 x 1.5 mm²
236 apertures in aluminum-coated polyimide tape. Each aperture can be identified by a unique
237 barcode milled on the tape. The tape is coated with a 50 nm-thick film (Luxel Corporation) that
238 spans the apertures and serves as support for sections. The steps to perform before imaging
239 every section include: deliver a new aperture into the field of view using the reel-to-reel system,
240 locate the aperture center using stage algorithmically, find the illumination center of the electron
241 beam (which is often off-center due to magnetic hysteresis from magnification change or
242 change in charge equilibrium state of the new aperture), adjust camera gain control, extract
243 ROI, and autofocus at high magnification. These are done for every aperture with a tissue
244 section, and typically take 2 - 3 minutes per aperture (Table 1). Software (Blade, Voxa Inc.) has
245 been developed that can control the Reel-to-reel system, GridStage, and TEM automatically.
246 The software has lower-level functions that execute each step in the workflow (e.g. travel to a
247 specific aperture in the GridTape reel, move the stage, adjust focus of the TEM). The low-level
248 software supports end-user scripting and control of application-specific microscope workflows
249 via the Blade API supplied to the user. Additionally, the Blade software allows initialization of
250 imaging remote control over IP of all operations and multiple user-defined imaging modes - e.g.
251 continuous batch imaging, re-imaging, and selective or random sampling.

252 The acquisition computer for each microscope has an intermediate storage of 16 - 32 TB
253 SSDs via a PCIe card with 4 USB3.0 ports, for ~24 hours of imaged data. Each USB port can
254 support up to 10 Gb/s of transfer speed. After caching on the temporary storage on SSD, the
255 data are then transferred via a 10 Gb/s network connection to an on-premise petascale cloud
256 storage in a separate building. Data transfer is done using CloudFiles (<https://github.com/seung-lab/cloud-files>).

258 In general, imaging rates (Fig. 1d, Table 1) are computed as the number of pixels that
259 are acquired in a given amount of time to image a section. Burst imaging rates are calculated
260 from the number of pixels in a frame over camera exposure time per frame (6,000 x 6,000 pixels
261 in 40 ms). Montage imaging rates are calculated from the total number of pixels of all images
262 (i.e. number of pixels in a tile multiplied by number of tiles) over time, from the first image to the

263 last image of a montage acquisition. Sources of overhead for montage imaging rates include
264 imaging, stage motion, beam deflection, computational overhead of the acquisition software,
265 and computing basic image statistics (Fig. 1d). Net imaging rates are computed from the same
266 number of pixels as in montage imaging rate, including all overhead from montage imaging, but
267 additionally includes overhead for section transition (e.g. low-magnification overview of sections
268 on GridTape, ROI extraction, autofocus, automatic beam centering). Effective imaging rates are
269 calculated from the total number of pixels of a montage acquisition with overlap pixels only
270 counted once, over the same overhead as in the net imaging rate. Time for a montage
271 acquisition varies from section to section by ~30 MPix/s (s.d.) depending on variable
272 computational overhead in the acquisition software. Peak imaging rate is taken from an
273 acquisition with the shortest imaging time. Average imaging rates are taken from a typical
274 production acquisition (an average of 10 or more acquisitions). Average transition time is the
275 average taken from 10 consecutive automatic acquisitions.

276 Imaging duty cycle is computed as the fraction of time for image acquisition (number of
277 tiles x exposure time per tile) out of total time per section. For example, at 3 nm/Pixel the image
278 acquisition time is 2.9 minutes (4,356 tiles at 40 ms per tile), which is 33.7% out of total time per
279 section (8.6 minutes). Similarly, the imaging duty cycle at 4 nm/Pixel is 31%. In comparison, the peak
280 performance of the previous state of the art system¹² has an imaging duty cycle of 15% (2,600 tiles
281 at 50 ms per tile out of 14 minutes of total time).

282

283 **Stitching and alignment.** Image stitching was performed with the AlignTK software¹⁰
284 (<https://mmbios.pitt.edu/aligntk-home>). Image alignment was performed with a custom software
285 pipeline²⁰.

286

287 **Table 1. Performance metric for bdTEMs.**

288

289 **Supplementary video 1.** Screen recording of an acquisition at a peak imaging rate.

290 **Supplementary video 2.** Aligned images across 55 sections acquired at 120 ms exposure time.

291 **Supplementary video 3.** Aligned images across 20 sections acquired at 40 ms exposure time.

292 <https://doi.org/10.6084/m9.figshare.21614058>

293

294

295 **Acknowledgments**

296 The Cricket system was initially prototyped and tested by Voxa with the Allen Institute for Brain
297 Science¹². We thank R. Clay Reid, Daniel J. Bumbarger, Wenjing Yin, Derrick Brittain, Marc
298 Takeno, Nuno Macarico da Costa, David Hildebrand for advice on microscopy and serial
299 sectioning setup; Stephan Y. Thibierge for help in the planning and construction of the TEM
300 facility; Lawrence Own and Teddy DeRego for their development and support in GridStage and
301 Cricket hardware and software; Wei-Chung Allen Lee and Jasper Phelps for advice on image
302 stitching; John Price for modification of ATUMtome. This work was supported by the NIH grants
303 1S10OD023602-01A1 and 1U19NS104648 and the Simons Collaboration on the Global Brain.
304 The authors acknowledge the use of Princeton's Imaging and Analysis Center, which is partially
305 supported through the Princeton Center for Complex Materials (PCCM), a National Science
306 Foundation (NSF)-MRSEC program (DMR-2011750).

307

308 **Author contributions**

309 C.S.O. and A.A.W. conceived the study. Z.Z. developed the conceptual framework for
310 quantifying the performance. D.W.T. and H.S.S. acquired funding and supervised. A.A.W.
311 planned the construction of the facility and managed the installation and testing of the first
312 instrument. A.A.W. registered and stitched the initial datasets. Z.Z., C.S.O., and R.A.K.
313 developed software for TEM imaging. Z.Z., A.A.W., and E.W.H. developed software and
314 hardware for serial sectioning. W.M.S. developed software for data transfer. Z.Z. performed
315 image stitching. Z.Z. and N.K. performed image alignment. Z.Z. acquired and analyzed data.
316 Z.Z. and C.S.O. carried out validation and evaluation. Z.Z. and H.S.S. drafted the manuscript
317 with input from all authors.

318

319 **Competing interest**

320 N.K. and H.S.S. disclose financial interests in Zetta AI LLC. C.S.O. and R.A.K. disclose financial
321 interests in Voxa. A.A.W. is a founder and owner of ariadne.ai ag (Switzerland).

322

323 **References**

- 324 1. Harris, K. M. *et al.* Uniform serial sectioning for transmission electron microscopy. *J. Neurosci.* **26**, 12101–12103 (2006).
- 325 2. Stevens, J. K., Davis, T. L., Friedman, N. & Sterling, P. A systematic approach to
326 reconstructing microcircuitry by electron microscopy of serial sections. *Brain Res.* **2**, 265–
327 293 (1980).
- 328 3. Harris, K. M. & Weinberg, R. J. Ultrastructure of synapses in the mammalian brain. *Cold Spring Harb. Perspect. Biol.* **4**, (2012).
- 329 4. White, J. G., Southgate, E., Thomson, J. N. & Brenner, S. The structure of the nervous
330 system of the nematode *Caenorhabditis elegans*. *Philos. Trans. R. Soc. Lond. B Biol. Sci.*
331 **314**, 1–340 (1986).
- 332 5. Cook, S. J. *et al.* Whole-animal connectomes of both *Caenorhabditis elegans* sexes. *Nature*
333 **571**, 63–71 (2019).
- 334 6. Witvliet, D. *et al.* Connectomes across development reveal principles of brain maturation.
335 *Nature* **596**, 257–261 (2021).

- 338 7. Eichler, K. *et al.* The complete connectome of a learning and memory centre in an insect
339 brain. *Nature* **548**, 175–182 (2017).
- 340 8. Sigulinsky, C. L. *et al.* Network Architecture of Gap Junctional Coupling among Parallel
341 Processing Channels in the Mammalian Retina. *J. Neurosci.* **40**, 4483–4511 (2020).
- 342 9. Pfeiffer, R. L. *et al.* A pathoconnectome of early neurodegeneration: Network changes in
343 retinal degeneration. *Exp. Eye Res.* **199**, 108196 (2020).
- 344 10. Bock, D. D. *et al.* Network anatomy and in vivo physiology of visual cortical neurons. *Nature*
345 **471**, 177–182 (2011).
- 346 11. Lee, W.-C. A. *et al.* Anatomy and function of an excitatory network in the visual cortex.
347 *Nature* **532**, 370–374 (2016).
- 348 12. Yin, W. *et al.* A petascale automated imaging pipeline for mapping neuronal circuits with
349 high-throughput transmission electron microscopy. *Nat. Commun.* **11**, 4949 (2020).
- 350 13. Phelps, J. S. *et al.* Reconstruction of motor control circuits in adult Drosophila using
351 automated transmission electron microscopy. *Cell* **184**, 759–774.e18 (2021).
- 352 14. Zheng, Z. *et al.* A Complete Electron Microscopy Volume of the Brain of Adult Drosophila
353 melanogaster. *Cell* **174**, 730–743.e22 (2018).
- 354 15. MICrONS Consortium *et al.* Functional connectomics spanning multiple areas of mouse
355 visual cortex. *bioRxiv* 2021.07.28.454025 (2021) doi:10.1101/2021.07.28.454025.
- 356 16. Mahalingam, G. *et al.* A scalable and modular automated pipeline for stitching of large
357 electron microscopy datasets. *Elife* **11**, (2022).
- 358 17. Abbott, L. F. *et al.* The mind of a mouse. *Cell* **182**, 1372–1376 (2020).
- 359 18. Shapson-Coe, A. *et al.* A connectomic study of a petascale fragment of human cerebral
360 cortex. Preprint at <https://doi.org/10.1101/2021.05.29.446289> (2021).
- 361 19. Macrina, T. *et al.* Petascale neural circuit reconstruction: automated methods. *bioRxiv*
362 2021.08.04.455162 (2021) doi:10.1101/2021.08.04.455162.
- 363 20. Popovych, S. *et al.* Petascale pipeline for precise alignment of images from serial section

364 electron microscopy. *bioRxiv* 2022.03.25.485816 (2022) doi:10.1101/2022.03.25.485816.

365 21. Hayworth, K. J. *et al.* Gas cluster ion beam SEM for imaging of large tissue samples with
366 10 nm isotropic resolution. *Nat. Methods* **17**, 68–71 (2020).

367 22. Templier, T. MagC, magnetic collection of ultrathin sections for volumetric correlative light
368 and electron microscopy. *Elife* **8**, (2019).

369 23. Soto, G. E. et al. Serial section electron tomography: a method for three-dimensional
370 reconstruction of large structures. *Neuroimage* **1**, 230–243 (1994).

371 24. Mikula, S. & Denk, W. High-resolution whole-brain staining for electron microscopic circuit
372 reconstruction. *Nat. Methods* **12**, 541–546 (2015).

373 25. Own, C. S. *et al.* Multi-order Scaling of High-throughput Transmission Electron Microscopy.
374 *Microsc. Microanal.* **25**, 1040–1041 (2019).

375

Fig. 1

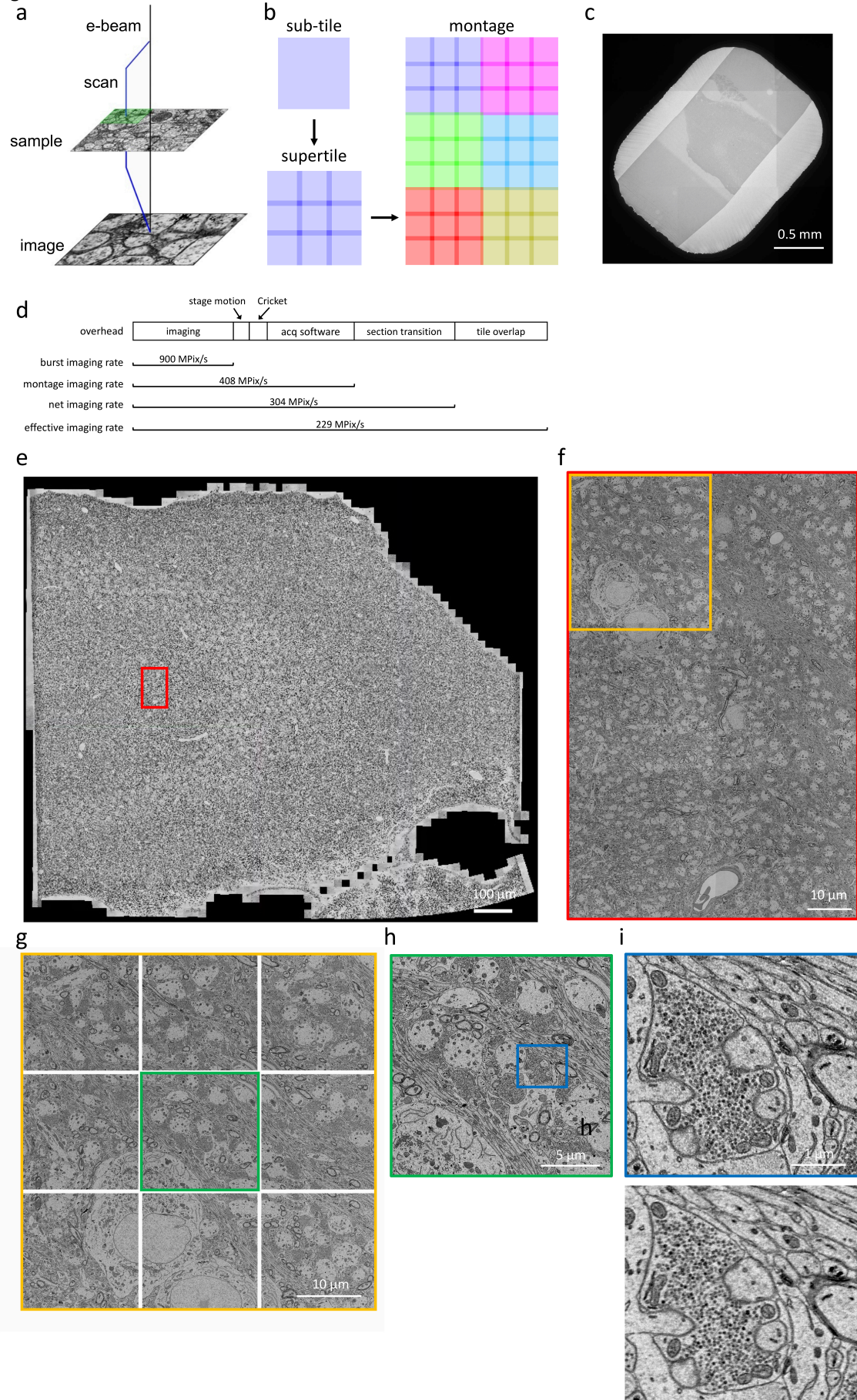


Fig. 1. Beam deflection for TEM imaging

a-b, Cricket Schematic. At a stage position, Cricket sequentially scans each tile of a 3 x 3 matrix pattern on the sample. The tiles can be stitched together in real-time, producing a “supertile”. Each square represents a single tile and 9 tiles compose a supertile with overlap between tiles. Neighboring supertiles (different colors) can be stitched together to form a montage image. **c**, Overview of a section on a 2 mm x 1.5 mm slot imaged using Cricket at low magnification. **d**, Imaging speed based on acquisitions at 3 nm/pix (*Methods*). The bar lengths are proportional to the contribution of each overhead to imaging speed. Computational overhead of acquisition (“acq software”) includes communications between different components, software time jitters, computing image statistics, on-the-fly stitching of subtiles to supertiles, and image storage. **e**, A fully stitched montage of a hippocampus section (1 mm²) imaged with a Cricket-equipped TEM. The montage includes 4320 tiles (or 480 supertiles). **f**, A montage of 6 stitched supertiles (from red outline in **e**). **g**, A Cricket supertile consisting of 9 tiles (from orange outline in **f**). Each tile has 6,000 x 6,000 pixels and the overlap between neighboring subtiles of a supertile is 15% (~900 pixels). **h**, A single image tile (from green outline in **g**). **i**, High-magnification EM images with 120 ms (upper, from blue outline in **h**) and 40 ms exposure time (lower).

Table 1
 bioRxiv preprint doi: <https://doi.org/10.1101/2022.11.23.517701>; this version posted November 24, 2022. The copyright holder for this preprint (which was not certified by peer review) is the author/funder, who has granted bioRxiv a license to display the preprint in perpetuity. It is made available under aCC-BY-NC-ND 4.0 International license.

imaging parameters	avg. 3 nm/pix (120 ms exp.)	avg. 3 nm/pix (40 ms exp.)	peak 3 nm/pix (40 ms exp.)	avg. 3.6 nm/pix (40 ms exp.)	unit
resolution	3	3	3	3.6	nm/pixel
tile size	6000	6000	6000	6000	pix (aspect ratio of 1:1)
FOV size	18	18	18	21.6	μm
pixels per tile	36	36	36	36	Mpixel
supertile size (per side, 15% overlap b/w tiles)	16200	16200	16200	16200	pix (aspect ratio of 1:1)
overlap between supertiles	600	600	600	600	pix (i.e. 10% of tile size)
exposure time	120	40	40	40	ms
tiles per section (w/ overlap)	4356	4356	4140	2916	tile
supertiles per section (w/ overlap)	484	484	460	324	supertile
imaging time per section	11.7	6.4	4.7	4	minute
transition overhead (tape translation, ROI definition, autofocus, etc.)	2.2	2.2	1.8	2.2	minute
total time per section	13.9	8.6	6.5	6.2	minute
burst imaging rate (imaging only)	900	900	900	900	Mpix/s
montage imaging rate (w/ stage, Cricket)	223	408	529	437	Mpix/s
net imaging rate (w/ stage, Cricket, transition)	188	304	382	282	Mpix/s
effective imaging rate (w/ stage, Cricket, transition, overlap)	142	229	288	213	Mpix/s
sections per day (1 scope at 24 hr)	103	167	221	232	section
time to image 1 mm ³ (4 scopes at 24/7)	54	34	26	24	days
time to image 1 mm ³ (4 scopes at 65% uptime #)	83	52	39	37	days

65% uptime accounts for microscope maintenance, imaging pause (Yin et al. 2020)

Extended Data Fig. 1

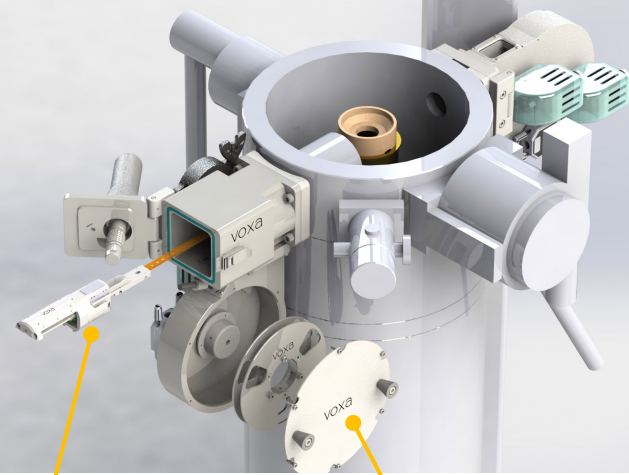
a



50 megapixel camera & lens system

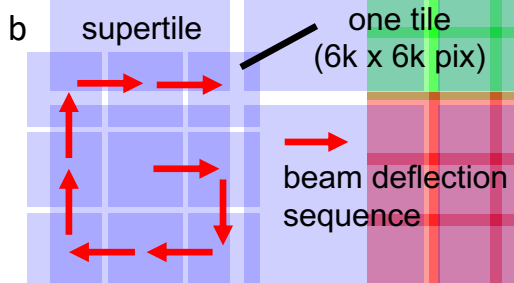
Cricket: beam scanner for TEM

GridStage: automated reel-to-reel system

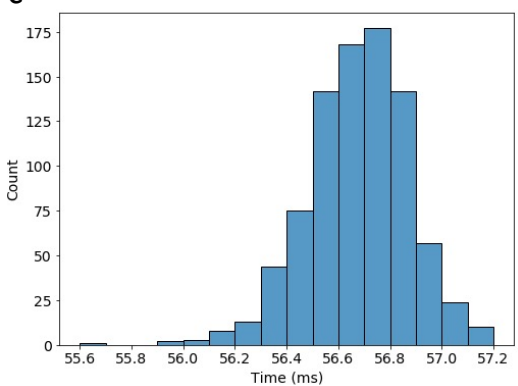


Cartridge: dual-axis piezo-driven fast stage

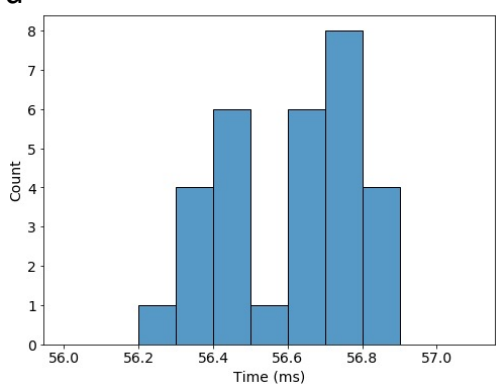
GridTape and housing



c



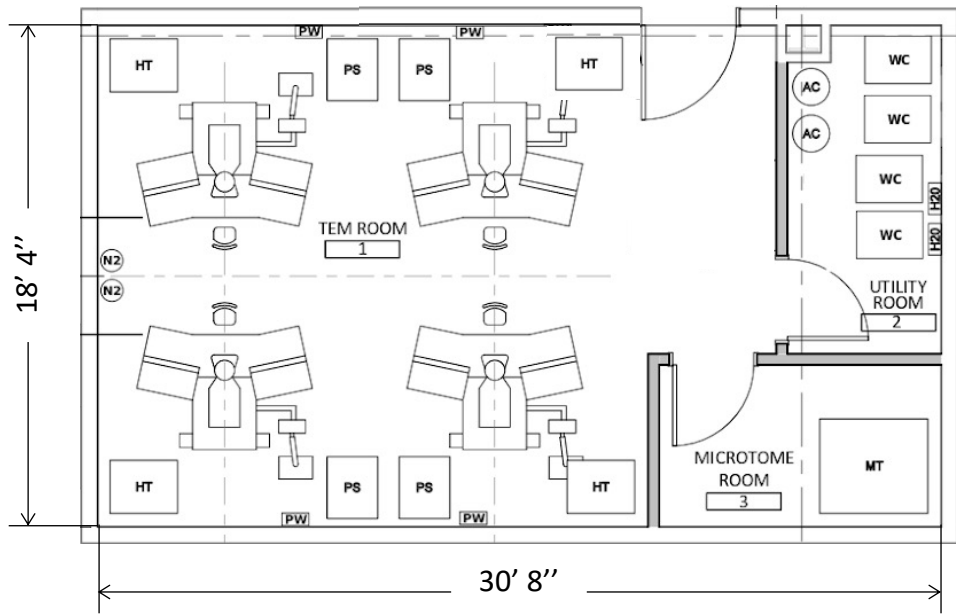
d



Extended Data Fig. 1. A bdTEM for high-throughput imaging.

a, The TEM is a refurbished JEOL 1200EX-II with 120 KV accelerating voltage. The custom modifications include a beam deflection mechanism (Cricket, Voxa), an advanced reel-to-reel tape translation system with a dual-axis piezo-driven fast stage (GridStage, Voxa), and a high speed CMOS camera (CB500MG-CM, XIMEA) with improved lens design (NanoSprint50M-AV, AMT). **b**, Scanning sequence of tiles in a supertile. **c-d**, Distributions of stage step-and-settle time in x (c) and y (d) axes.

a



b



Extended Data Fig. 2. A bdTEM facility.

a, Dimensions of a microscope room that houses an array of 4 bdTEMs with an inside room for sectioning.
b, A photograph of 4 bdTEMs that are installed in the same microscope room (a).